

## HEMISPHERE DIELECTRIC RESONATOR PATTERN RECONFIGURABLE ANTENNA AND ITS LINEAR PHASED ARRAY

Z.-F. Ding, S.-Q. Xiao, Y.-Y. Bai, and B.-Z. Wang

Institute of Applied Physics  
University of Electronic Science and Technology of China  
Chengdu 610054, P. R. China

**Abstract**—A hemisphere dielectric resonator pattern reconfigurable antenna (DRA) is proposed in this paper. The proposed antenna element can operate in four states (SI~SIV) and correspondingly reconfigure its patterns in four directions. A thinning linear array by non-uniform spacing with the element is constructed to scan its main beam from  $\theta = -77^\circ$  to  $77^\circ$  in  $E$ -plane with 3-dB beam coverage from  $\theta = -90^\circ$  to  $90^\circ$  by changing two states and progressive phases.

### 1. INTRODUCTION

In the modern communication and radar systems, antennas are often required to transmit signal in different directions. Phased array [3–5] can electronically control its main beam by adjusting the excited phase of the elements, which results in its extensive applications. However there are two key factors which limit the pattern scanning ability of the phased array. One is the mutual coupling between elements and the other is the inherent directivity of the element pattern [2]. Some effective technologies have been developed to suppress the element mutual coupling in array design [4–7]. Recently, one attempt has used the reconfigurable antenna as element in the phased array design [6–8]. The pattern reconfigurable antenna can reconfigure its pattern, thus, when it is used as an array element the pattern scanning ability of the phased array can be improved because an additional degree of freedom is added.

In this paper, a hemisphere dielectric resonator (DRA) [9–11] pattern reconfigurable antenna [12–14] is presented. The antenna

---

Corresponding author: S.-Q. Xiao (xiaoshaoqiu@uestc.edu.cn).

can operate in four states (SI~SIV) and accordingly reconfigure its pattern in four mutual perpendicular directions. Then a thinning linear array [15–17] with non-uniform spacing is constructed using such elements. The studied results indicate that the array can scan its main beam from  $\theta = -77^\circ$  to  $77^\circ$  in  $E$ -plane with 3-dB beam coverage from  $\theta = -90^\circ$  to  $90^\circ$  by shifting the states of the reconfigurable elements and progressive phases. Another outstanding advantage is that the proposed array has ultralow grating lobes.

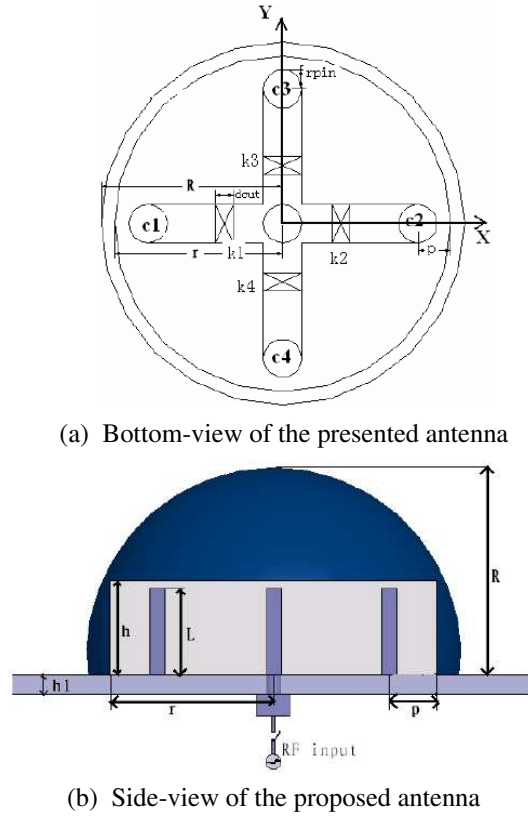


**Figure 1.** Geometry of the antenna element.

## 2. HEMISPHERE DIELECTRIC RESONATOR PATTERN RECONFIGURABLE ANTENNA ELEMENT

### 2.1. Geometry of the Antenna Element

The presented dielectric resonator antenna with a bottom foam layer (relative permittivity  $\epsilon_r = 1$ ) is shown in Fig. 1. The dielectric hemisphere has a relative permittivity of  $\epsilon_r = 6$ , a radius  $R = 7.2$  mm and a height  $h = 3.5$  mm, respectively. An inner cylinder with a radius of  $r = 6.6$  mm is removed and re-filled by a foam cylinder with the same shape. Four metal electrodes ( $c1 \sim c4$ ) are inserted into the foam cylinder and  $p = 1.1$  mm away from the edge of the foam cylinder. The metal electrodes are distributed symmetrically on the circle and have a radius of  $r_{\text{pin}} = 0.62$  mm and a length of  $L = 3.48$  mm. Four microstrip branch lines are etched on the surface of the dielectric substrate and connected with the four metal electrodes, respectively. Another port of each branch is joined together and then connected with the feed probe. The coaxial feed line has a characteristic impedance of  $50 \Omega$ . Four gaps with a width of  $d_{\text{cut}}$  are cut on the four microstrip branches. Four switches, i.e.,  $k1$ ,  $k2$ ,  $k3$  and  $k4$ , are installed in the four gaps, respectively. The ground plate has an area of  $2.1\lambda_0 \times 2.1\lambda_0$ , where  $\lambda_0$  is free space wavelength at operate frequency.

According to the pin diode (MA4GP905), when the bias is null, the diode operates as a low capacitance of  $0.025$  pF, and when a forward bias is applied to the diode, it can be equivalent to a low resistance of  $3 \Omega$ . Thus, for closely simulating the real switches, we substitute  $C_{\text{load}} = 0.025$  pF and  $R_{\text{load}} = 3 \Omega$  for the open and close states of the switches, respectively. By opening or closing those switches, four radiation patterns can be obtained. When  $k1$  is closed and others are opened, the antenna operates in so called state SI. When  $k2$  is closed and others are open, the antenna operates in so called state SII. And so on, the states SIII and SIV are obtained, too.

### 2.2. Simulation Results

The antenna is designed using the three-dimension high frequency EM simulation software HFSS10. The simulated return losses ( $S_{11}$ ) of the antenna element in states SI and SII are shown in Fig. 2. The results indicate that the antenna can operate well around  $10.04$  GHz in the two states. Fig. 3 shows the simulated radiation patterns in the  $E$ -plane at states SI and SII. It can be observed that the main beam of the antenna can be scanned in  $E$ -plane by switching the antenna states between states SI and SII. The main beam direction and the corresponding half power beam coverage in  $E$ -plane ( $xoz$ ) are (SI,  $-44^\circ$ ,  $-13^\circ \sim -75^\circ$ ),

(SII,  $45^\circ$ ,  $12^\circ \sim 76^\circ$ ). As our expectation, the patterns of the two states are symmetrical, and the corresponding characteristics of states SIII and SIV can be obtained too. For simplification, the characteristics of states SIII and SIV are not listed here.

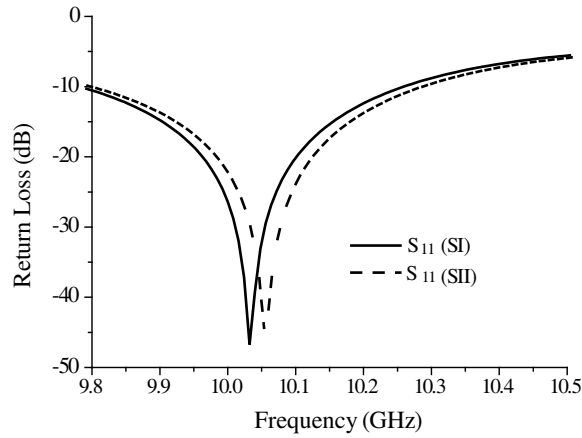
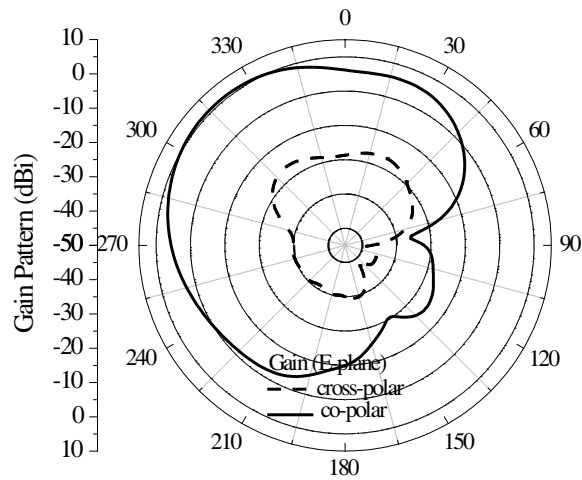
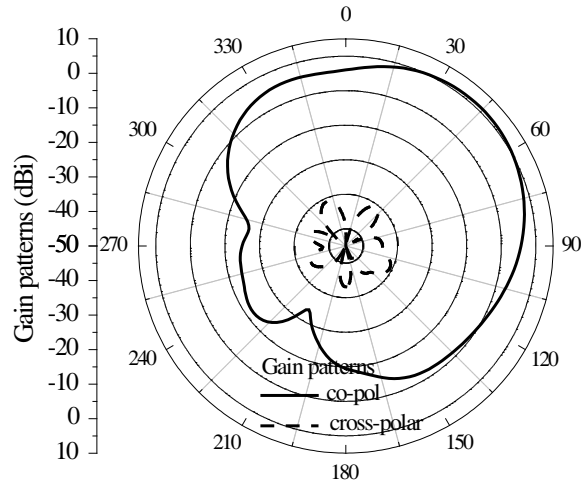


**Figure 2.** Simulated return loss for this antenna.



(a) state SI



(b) state SII

**Figure 3.** Simulated radiation patterns in the *E*-plane at two states for this antenna element.

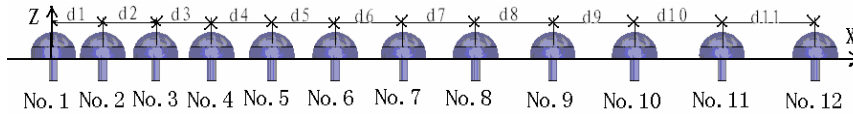


**Figure 4.** Configuration of the linear phased array.

### 3. LINEAR PHASED ARRAY WITH RECONFIGURABLE ANTENNA ELEMENTS

For avoiding the appearance of grating lobes and reducing the mutual coupling between adjacent elements, thinning array by non-uniform spacing is adopted to study the performance of the linear phased array with the proposed reconfigurable antenna elements. Fig. 4 shows the configuration of the proposed linear phased array. Twelve elements, named No. 1–No. 12, are arranged along *x*-axis with different spacing ( $d_1 \sim d_{11}$ ) and all of the elements operate in the same state. In this paper, we study only state SI. Element position  $x_n$  is represented as follow formula:

$$x_n = \sum_0^{N-1} d_n = \frac{L}{r-1} \left( r^{\frac{n-1}{N-1}} - 1 \right) \quad (1)$$

where  $r = d_{11}/d_1$ ,  $n$  is the  $n$ th element,  $N$  is the amount of elements of the array,  $L$  is the total length of the linear array; in this array, we choose  $L = 8\lambda_0$ . When the array scans in  $E$ -plane, each element's port exciting phase is

$$\Delta\varphi_n = \frac{2\pi}{\lambda_0} x_n \cdot \sin(\theta_0) \quad (2)$$

where  $\theta_0$  is the scan main beam direction of the array. The simulated return losses of each port and mutual coupling between two adjacent elements are shown in Fig. 5. In this figure, it can be observed that

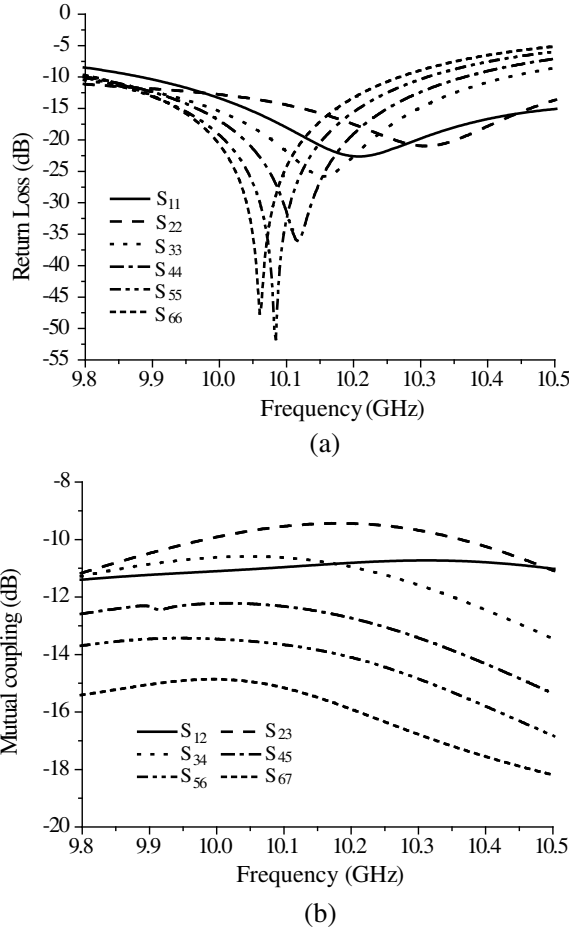


**Figure 5.** Simulated (a) return loss of each port and (b) mutual coupling between adjacent elements.

at the operation frequency of 10.04 GHz the biggest return loss is  $-15$  dB and it belongs to element No. 2 and a mutual coupling of less than  $-10$  dB is obtained between the adjacent elements. The studies also demonstrate that the mutual coupling between other elements gradually decrease with increased spacing  $d_n$  due to the thinning arrangement of the array.

The radiation characteristics of the non-uniform spacing phased array are analyzed. The array can scan its patterns in  $E$ -plane (i.e.,  $\varphi = 180^\circ$ ) by changing the progressive phase  $\Delta\psi$ , and the results are shown in Fig. 6. The array can scan its main beam from  $\theta = 0^\circ$  to  $-77^\circ$  in  $E$ -plane ( $\varphi = 180^\circ$ ) with 3 dB beam coverage getting to  $\theta = -90^\circ$  and without grating lobes. The detailed data is shown in Table 1. According to the symmetry characteristic of states SI and SII, the array can scan in  $E$ -plane ( $\varphi = 0^\circ$ ) from  $\theta = 0^\circ$  to  $\theta = 90^\circ$ . So the array can scan above the  $xoz$ -plane (i.e.,  $\theta = -90^\circ \sim 90^\circ$ ,  $\varphi = 0^\circ$ ) by reconfiguring the array operate states between states SI and SII and changing progressive phase.

According to the same characteristics of the antenna element four states, the other thinning array by non-uniform spacing can be designed with the elements being arranged along  $y$ -axis, the array can scan above the  $yo z$ -plane (i.e.,  $\theta = -90^\circ \sim 90^\circ$ ,  $\varphi = 90^\circ$ ) by reconfiguring the array operate states between states SIII and SIV and changing progressive phase.

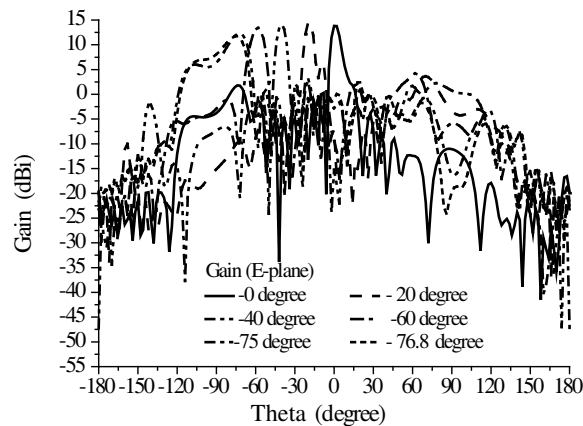


**Figure 6.** Radiation patterns of the proposed array with various progressive phased.

**Table 1.** Array pattern characteristics in  $E$ -plane of state SI with various progressive phases.

Beam direction ( $\theta^\circ$ , $180^\circ$ )	3 dB beam coverage	Gain (dBi)
( $0^\circ$ , $180^\circ$ )	( $-1^\circ$ , $5^\circ$ )	13.95
( $-10^\circ$ , $180^\circ$ )	( $-6^\circ$ , $-12^\circ$ )	15.12
( $-20^\circ$ , $180^\circ$ )	( $-15^\circ$ , $-22^\circ$ )	14.51
( $-30^\circ$ , $180^\circ$ )	( $-27^\circ$ , $-34^\circ$ )	13.49
( $-40^\circ$ , $180^\circ$ )	( $-36^\circ$ , $-44^\circ$ )	14.12
( $-50^\circ$ , $180^\circ$ )	( $-44^\circ$ , $-54^\circ$ )	13.89
( $-60^\circ$ , $180^\circ$ )	( $-53^\circ$ , $-64^\circ$ )	13.42
( $-68^\circ$ , $180^\circ$ )	( $-66^\circ$ , $-76^\circ$ )	13.21
( $-72^\circ$ , $180^\circ$ )	( $-66^\circ$ , $-83^\circ$ )	12.31
( $-77^\circ$ , $180^\circ$ )	( $-68^\circ$ , $-90^\circ$ )	11.71

#### 4. CONCLUSION

A new hemisphere dielectric resonator antenna with four reconfigurable operating states and four patterns is presented in this paper. A thinning linear array by non-uniform spacing with the proposed elements is designed to scan its main beam from  $\theta = -77^\circ$  to  $77^\circ$  in  $E$ -plane with 3-dB beam coverage from  $\theta = -90^\circ$  to  $90^\circ$  by changing two states and progressive phases.

#### ACKNOWLEDGMENT

This work was in part supported by aviation Science foundation under grant 20070180003, in part by the new-century talent program of the education department of China under grant NCET070154, in part by national defense research funding under grant PJ08DZ0229 and in part by the national natural science foundation of China under grant No. 60872034.

#### REFERENCES

1. Garg, R., P. Bhartia, I. Bahl, and A. Ittipiboon, *Microstrip Antenna Design Handbook*, Artech House, Norwood, MA, 2001.



2. Fallahi, R. and M. Roshandel, "Effect of mutual coupling and configuration of concentric circular array antenna on the signal-to-interference performance in CDMA systems," *Progress In Electromagnetics Research*, PIER 76, 427–447, 2007.
3. Staraj, R., E. Cambiaggio, and A. Papiernik, "Infinite phased arrays of microstrip antennas with parasitic elements: Application to bandwidth enhancement," *IEEE Trans. on Antennas and Propagation*, Vol. 42, No. 5, 742–746, 1994.
4. Skrivervic, A. K. and J. R. Mosig, "Finite phased array of microstrip patch antennas: The infinite array approach," *IEEE Trans. on Antennas and Propagation*, Vol. 40, No. 5, 579–582, 1992.
5. Javier, G. T., F. W. Parveen, T. C. Michael, and G. C. Christos, "FDTD analysis of finite-sized phased array microstrip antennas," *IEEE Trans. on Antennas and Propagation*, Vol. 51, No. 8, 2057–2062, 2003.
6. Yang, X.-S. and B.-Z. Wang, "Yagi patch antenna with dual-band and pattern reconfigurable characteristics," *IEEE Antenna and Wireless Propagation Letters*, Vol. 6, 168–171, 2007.
7. Zhang, S., G. H. Huff, et al., "A pattern reconfigurable microstrip parasitic array," *IEEE Trans. on Antennas and Propagation*, Vol. 52, No. 10, 2773–2776, 2004.
8. Wu, S.-J. and T.-G. Ma, "A wideband slotted bow-tie antenna with reconfigurable CPW-to-slotline transition for pattern diversity," *IEEE Trans. on Antennas and Propagation*, Vol. 56, No. 2, 327–334, 2008.
9. Saed, M. and R. Yadla, "Microstrip-fed low profile and compact dielectric resonator antenna," *Progress In Electromagnetics Research*, PIER 56, 151–161, 2006.
10. Rezaei, P., M. Hakkak, and K. Forooraghi, "Design of wideband dielectric resonator antenna with a two-segment structure," *Progress In Electromagnetics Research*, PIER 66, 111–124, 2006.
11. Kumar, A. V. P., V. Hamsakutty, J. Yoyannan, and K. T. Mathew, "Micro-strip fed cylindrical dielectric resonator antenna with a coplanar parasitic strip," *Progress In Electromagnetics Research*, PIER 60, 143–152, 2006.
12. Mongia, R. K., A. Ittipibon, and M. Cuhaci, "Measurement of radiation efficiency of dielectric resonator antennas," *IEEE Microwave Guided Wave. Lett.*, Vol. 4, 80–82, 1994.
13. Kishk, A. A., "Wideband dielectric resonator antenna in truncated tetrahedron from excited by a coaxial probe," *IEEE*

- Trans. on Antennas and Propagation*, Vol. 51, No. 10, 2913–2917, 2003.
14. Kishk, A. A., Y. Yin, et al., “Conical dielectric resonator antennas for wideband application,” *IEEE Trans. on Antennas and Propagation*, Vol. 50, No. 4, 469–474, 2002.
  15. Zhang, Y. and B. Zhu, “Study of optimum thinning arrays by non-uniform spacing,” *ACTA ELECTRONICA SINICA*, Vol. 17, No. 4, 81–87, 1989.
  16. Haupt, R. L., “Thinned arrays using genetic algorithms,” *IEEE Trans. on Antennas and Propagation*, Vol. 42, No. 7, 993–999, 1994.
  17. Razavi, A. and K. Forooraghi, “Thinned arrays using pattern search algorithms,” *Progress In Electromagnetics Research*, PIER 78, 61–71, 2008.